

AN EXPERIMENTAL STUDY FOR THE PREDICTION
OF PRESSURE LAG INHERENT IN
BALLISTIC MISSILE PLUMBING SYSTEMS
WHEN SUBJECTED TO CONTINUOUS-TYPE
PRESSURE FUNCTIONS

A THESIS

Presented to
the Faculty of the Graduate Division
by
Robert Smith Hiers, Jr.

In Partial Fulfillment
of the Requirements for the Degree
Master of Science in Aeronautical Engineering

Georgia Institute of Technology

August, 1959

"In presenting the dissertation as a partial fulfillment of the requirements for an advanced degree from the Georgia Institute of Technology, I agree that the Library of the Institution shall make it available for inspection and circulation in accordance with its regulations governing materials of this type. I agree that permission to copy from, or to publish from this dissertation may be granted by the professor under whose direction it was written, or, in his absence by the dean of the Graduate Division when such copying or publication is solely for scholarly purposes and does not involve potential financial gain. It is understood that any copying from, or publication of, this dissertation which involves potential financial gain will not be allowed without written permission

52
12R-1

AN EXPERIMENTAL STUDY FOR THE PREDICTION
OF PRESSURE LAG INHERENT IN
BALLISTIC MISSILE PLUMBING SYSTEMS
WHEN SUBJECTED TO CONTINUOUS-TYPE
PRESSURE FUNCTIONS

Approved:

Date Approved by Chairman: September 8, 1959

ACKNOWLEDGMENTS

The author is deeply indebted to Dr. Arnold L. Ducoffe for his suggestion of the topic and the extensive work rendered throughout the experimentation. For their critical review of the subject, the author is also indebted to Dr. Thomas W. Jackson and Dr. Frank M. White. The assistance of Mr. John Van Tassel during the experimentation, and the labors of Miss Barbara J. Daniels in the reduction and presentation of the data, are also appreciated.

Sincere appreciation is extended to the Army Ballistic Missile Agency, Huntsville, Alabama, for the financial and material aid which made this work possible.

TABLE OF CONTENTS

	Page
ACKNOWLEDGMENTS	ii
LIST OF FIGURES	iv
LIST OF SYMBOLS	v
SUMMARY	vi
Chapter	
I. INTRODUCTION	1
II. APPARATUS	4
III. PROCEDURE	10
IV. RESULTS	18
V. CONCLUSIONS	27
VI. RECOMMENDATIONS	28
REFERENCES	29

LIST OF FIGURES

Figure		Page
1.	Schematic of Apparatus Used to Produce Continuous Input Pressure Functions	5
2.	Detail of Piston and Cylinder Assembly	6
3.	Typical Continuous Ascent Trajectories	13
4.	Typical Continuous Descent Trajectories	14
5.	Typical Descent Oscillograph Record	16
6.	System Parameter, K , as a Function of Geometric Parameter, \emptyset	20
7.	Correlation of Experiment with Theory for Continuous Descent Trajectory No. 3 and $\emptyset = 80.49$	22
8.	Correlation of Experiment with Theory for Continuous Descent Trajectory No. 3 and $\emptyset = 76.55$	23
9.	Correlation of Experiment with Theory for Continuous Ascent Trajectory No. 2 and $\emptyset = 46.25$	24
10.	Correlation of Experiment with Theory for Continuous Ascent Trajectory No. 3 and $\emptyset = 1257$	25
11.	Correlation of Experiment with Theory for Continuous Descent Trajectory No. 3 and $\emptyset = 482.5$	26

LIST OF SYMBOLS

d	inside diameter of tubing in inches
K	system parameter
L	length of tubing in inches
L/d	tubing length to diameter ratio
mm Hg	millimeters of mercury
p	pressure
$p(t)$	transient input pressure
p_1	transient response pressure
p_i	transient input pressure
p_r	transient response pressure
Δp	pressure difference or pressure lag
psi	pressure in pounds per square inch
r.m.s.	root mean square
rpm	revolutions per minute
sec	seconds
t	time in seconds
T	absolute temperature
V	total volume of system
V_s	total sensing volume
λ	time lag constant
μ	coefficient of viscosity

SUMMARY

This investigation presents the results of an experimental study of the pneumatic pressure lag inherent in typical missile plumbing systems when subjected to continuous-type transient input pressure functions during ascending and descending flight.

Experimental tests were run for various system geometries using line length, line diameter, and sensing volume as variables. Four line lengths, 75, 60, 45, and 30 inches, four line diameters, 1/16, 1/8, 5/32, and 3/16 inch, and five sensing volumes, 1.7, 5, 10, 20, and 40 cubic inches, and all combinations thereof were used in the experimentation. In addition, five descent and three ascent input pressure functions were used to simulate the ascending and descending flight of typical missiles.

The apparatus used to produce the various trajectories consisted of a cam-piston arrangement which allowed air to be bled into or out of the line and sensing volume at any desired rate. The shape and rate of travel of the cam were adjusted experimentally until the desired trajectories were simulated.

The pneumatic pressure lag was measured with a differential transducer located between the sensing volume and input end of the line. The input pressure was measured with six absolute transducers located at the input end of the tubing.

The results of this experiment were correlated with a theory

which assumes a quasi-steady, fully-developed, laminar, tube flow with isothermal changes of state.

An empirically determined system parameter, which is shown to be a function of system geometry and independent of trajectory, is presented. The resulting correlation between theory and experiment is very good.

The results of this analysis are limited to a simple series system having a constant area line and a sensing volume. Further investigation of the effects of inlet temperature and connector fittings having inside diameters smaller than the tube diameter is considered necessary for the complete solution of the use of plumbing systems for the measurement of pressure.

CHAPTER I

INTRODUCTION

The measurement of transient-input pneumatic pressure by means of a series system comprised of constant area tubing attached to a sensing volume has been the subject of numerous investigations during the past twenty-five years.

The early attempts (References 1, 2 and 3) to predict pneumatic pressure lag were concerned primarily with the measurement of pitot tube static pressures for aircraft whose speeds lay in the 200 - 400 MPH category. In this velocity regime the transients encountered during maneuvering or diving flight were small in nature so that the pneumatic pressure lag could be predicted to a reasonable degree of accuracy by a mathematical model in the form of a first order linear differential equation; namely,

$$\lambda \frac{dp_1}{dt} + p_1 = p(t) \quad (1)$$

where λ is a lag time constant, p_1 is the pressure in the sensing volume, $p(t)$ is the transient-input pressure function, and t is time.

The introduction of transonic and supersonic aircraft and high speed missiles following World War II resulted in transient-input pressures which could not be represented by Equation (1). During this period, Vaughn (Reference 4) developed a non-linear theory based upon the mass

flow through a sharp-edged orifice attached to a sensing volume. The resulting mathematical expression is given as

$$\frac{dp_1}{dt} = \frac{T_1}{T} B \sqrt{p^2 - p_1^2} \quad (2)$$

where p_1 is the sensing volume pressure, p is the transient input pressure, T_1 is the absolute temperature in the sensing volume, T is the absolute input temperature, and B is a function of the system geometry and input temperature. Equation (2) appears to give satisfactory results for systems with short line lengths subjected to small impulse input pressures, but for systems comprised of long lines and subjected to high rate transient input pressures, the use of Equation (2) results in doubtful correlation of theory with experiment.

Recently, a theory (Reference 5) assuming a quasi-steady, fully-developed, laminar, isothermal tube flow for predicting pneumatic pressure lag in simple series systems, has been developed. The resulting expression for the pressure lag is given as

$$\frac{dp_r}{dt} = \frac{\pi d^4}{256\mu VL} (p_i^2 - p_r^2) \quad (3)$$

where d is the diameter of the tubing, μ is the viscosity coefficient, V is the total volume of the system, L is the length of the tubing, p_i is the transient input pressure, p_r is the pressure in the sensing volume, and t is time.

The purpose of this investigation is to determine experimentally

the values of the system parameter, $K = \frac{\pi d^4}{256\mu VL}$, appearing in Equation (3), and then to compare theoretically calculated values of the pressure lag, $\Delta p = p_i - p_r$, with those obtained experimentally.

CHAPTER II

APPARATUS

The main components of the apparatus are shown in Figure 1 and consist of the test tube, the sensing volume, the cam-piston assembly, the absolute and differential pressure transducers, the gear reduction assembly, the synchronous drive motor, and the recording and amplifying equipment.

Piston-Cylinder Assembly.--Figure 2 is a detail view of the piston-cylinder assembly showing the approximate dimensions of the components in inches. The piston is divided into three sections by means of rubber O-rings. The two O-rings, located to the left, seal the cylinder from the atmosphere. The O-ring on the right side prevents any air flow between the vacuum or high pressure source and the test section. Thus, the only manner in which air can flow between the tankage and test section is through the inside of the piston and through the piston orifice when the piston orifice is moved to the right of the O-ring seal.

Cam.--The cam shown in Figure 1 is attached to a rack and is driven by a synchronous motor which is geared to a speed reducer. The shape of the cam was determined experimentally so that it produced the desired input pressure functions.

Gear Reduction.--The gear reduction arrangement consisted of a commercial

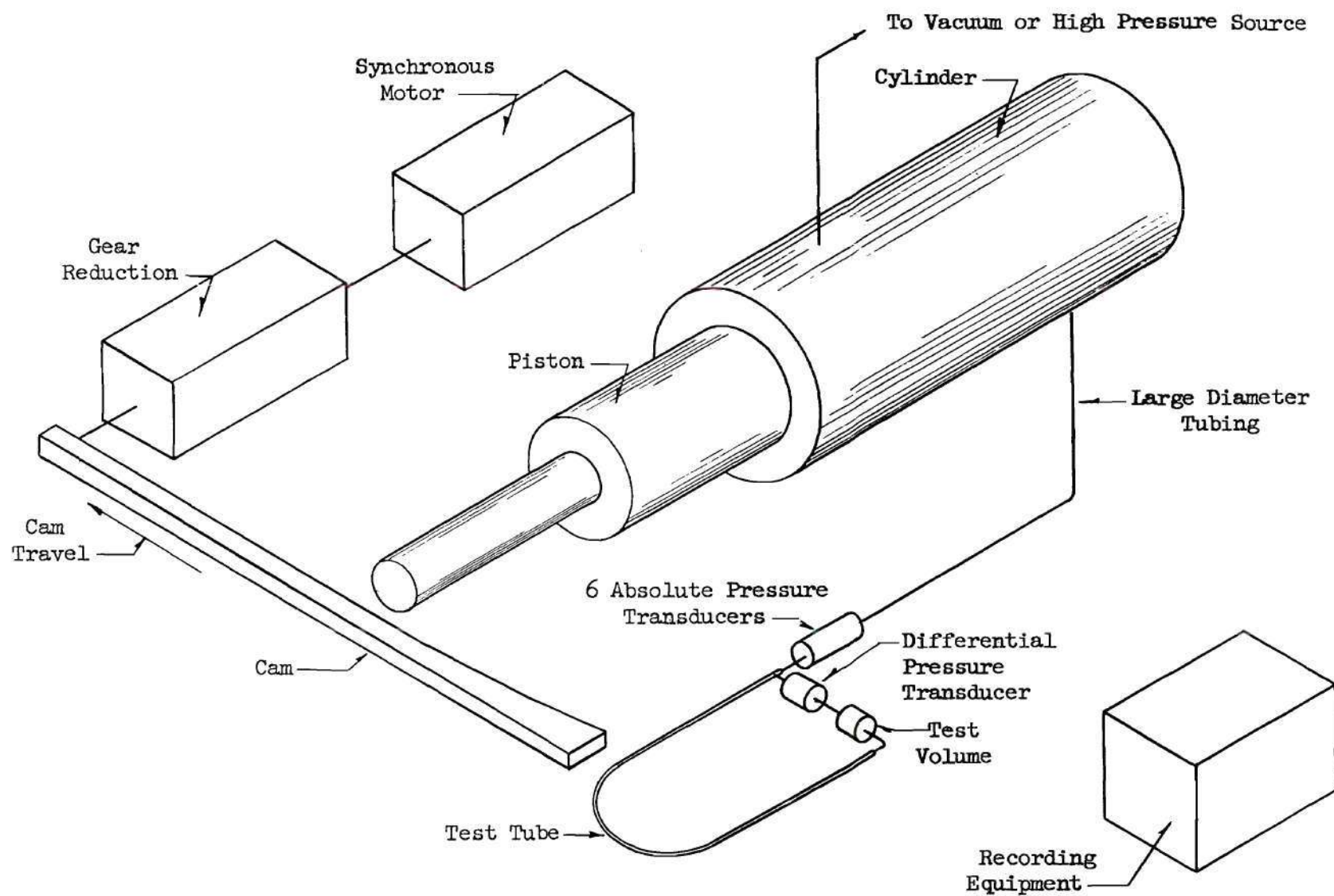


Fig. 1. Schematic of Apparatus Used to Produce Continuous Input Pressure Functions.

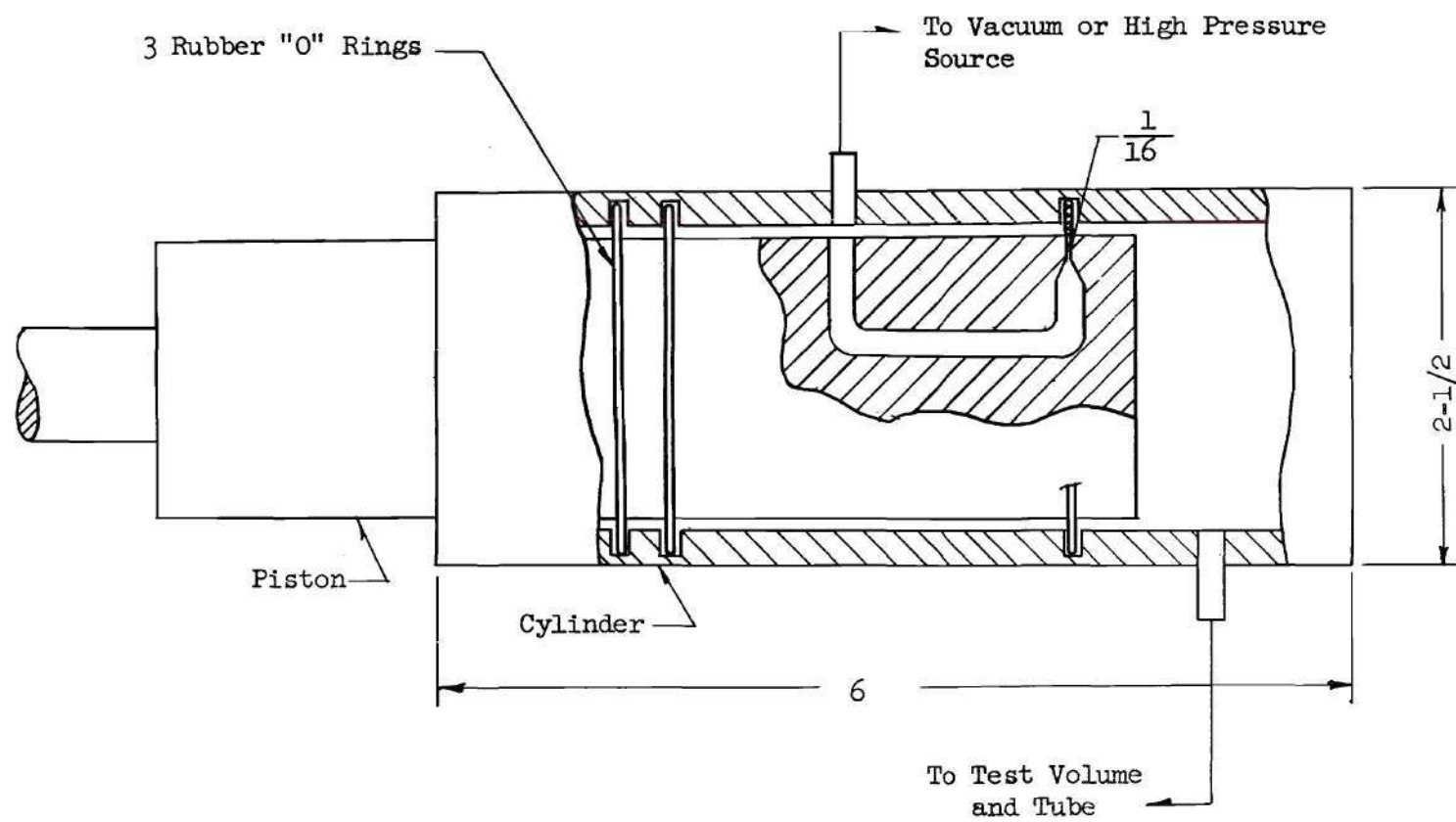


Fig. 2. Detail of Piston and Cylinder Assembly.

900:1 gear reducer plus an adjustable gear assembly made with interchangeable gears, which allowed up to approximately 10:1 reduction. The gears in this adjustable assembly were changed so that eight different time-pressure trajectories, five descent and three ascent, could be simulated.

Synchronous Motor.--An 1800 rpm synchronous motor was used to drive the system at constant speed. This insured repeatability of the trajectories.

Vacuum and High Pressure Source.--The vacuum and high pressure sources, indicated in Figure 1, consisted of two 8000 cubic inch tanks connected in series. These tanks were either pressurized or evacuated, depending on whether an ascent or descent run was being made. Three commercial vacuum pumps were used to rapidly evacuate the tanks. For ascent runs, the tanks were pumped down to approximately 1 mm Hg absolute pressure, and for descent runs they were pressurized at 500 mm Hg gauge pressure.

Transducers.--The input pressures were measured by means of six absolute pressure transducers. The pressure difference between the input end of the tube and the sensing volume was measured by means of a differential transducer. The six absolute transducers and their ranges were: 0 - 15B* (740 mm Hg to 300 mm Hg), 0 - 15A (360 mm Hg to 170 mm Hg), 0 - 10 (230 mm Hg to 90 mm Hg), 0 - 5B (100 mm Hg to 30 mm Hg), 0 - 5A (40 mm Hg to 10 mm Hg), and 0 - 2 (15 mm Hg to 0). The use of overlapping transducer ranges was necessary for added sensitivity and maximum accuracy with the

*A and B are symbols used to denote levels of transducer range.

available equipment. The useful range of pressure difference for the differential transducer was ± 25 mm Hg. The input voltage to the absolute pressure transducers was held constant at 7.0 volts r.m.s. by resistances in series with a 10 volt source from the power supply. The differential transducer input voltage was held constant at 10 volts r.m.s.

Power Supply and Recording Equipment.--The electronic recording equipment consisted of an oscillator-power supply combination, seven separate amplifiers, and a recording oscillograph.

The oscillator-power supply combination provided the filament current, the regulated plate voltage, and a three kilocycle carrier frequency for the amplifiers. The power supply also supplied the exciting voltage for the absolute and differential pressure transducers.

The output signals from the seven pressure transducers were fed into separate amplifiers. The basic components of each amplifier were the balancing portion of the transducer bridge network, an attenuator, a three kilocycle carrier amplifier, and a demodulator. In applications of this type, the frequency response of the amplifiers is flat in the range of 0 - 600 cycles per second.

The output signals from the seven amplifiers were impressed on separate galvanometers in the recording oscillograph. The frequency response of the galvanometers was flat in the range of 0 - 1000 cycles per second. The optical distance from the galvanometers to the recording film was 11.5 inches. The recording film was stored in spool type magazines and was run at an approximate speed of one inch per second.

A synchronous motor in the oscillograph regulated the occurrence of the time-line traces on the recording film.

Test Tubes.--The seamless steel test tubes used in the experiment were bent in the form of a "U" with a 3-1/2 inch radius. Four lengths of tubing, 30, 45, 60, and 75 inches, with four inside diameters, 1/16, 1/8, 5/32, and 3/16 inch were tested. Any effects in the experimental results, due to the curvature of the U-tube, were considered insignificant because the air velocities in the tubing were small.

Sensing Volume.--Five sensing volumes, 1.7, 5, 10, 20, and 40 cubic inches were tested. The volumes were cylindrical in shape and coated with glyptal to prevent leaks. The differential transducer has a volume of 1.7 cubic inches. Thus, the four remaining volumes were constructed less this amount so that the total sensing volumes would be 1.7, 5, 10, 20, and 40 cubic inches.

System Tubing.--All tubing sizes are given by inside diameter. Three types of tubing were used between the component parts of the system: 1/4 and 5/16 inch flexible rubber vacuum hose, 3/8 inch copper tubing, and 1/2 inch flexible copper tubing. All metal to metal connections between tubing were soldered and coated with glyptal, and metal to hose connections were clamped and coated with glyptal.

Valves.--To check for leaks and to isolate various sections of the system during operation, valves and rubber hose screw clamps were conveniently placed throughout the system.

CHAPTER III

PROCEDURE

The main steps of the daily test procedure began with the calibration of the absolute and differential transducers. Following the calibrations, the two 8000 cubic inch tanks were pumped down to about 1 mm Hg absolute for an ascent run, or pressurized to 500 mm Hg gauge pressure for a descent run. After several preliminary checks consisting of testing the system for air leaks and adjusting the amplifiers and recorders, the system was ready for a test run. The details of the main steps are included in the following description of the test procedure.

Calibration of Absolute Pressure Transducers.--The calibration of the absolute pressure transducers was accomplished with the use of four absolute pressure gauges having ranges of 0 - 20 mm Hg, 0 - 100 mm Hg, 0 - 400 mm Hg and 400 - 800 mm Hg, absolute. These gauges had previously been calibrated against an Arrowsmith gauge. The transducers were calibrated using pressure variations in the same direction as would be encountered during the experimentation, thus minimizing the hysteresis errors. The range and estimated error of each transducer are shown in Table 1. The full range of each transducer was spread over five inches of recorder film.

Calibration of Differential Pressure Transducer.--The differential transducer was calibrated by use of an alcohol manometer, sensitive to ± 1 mm

Table 1. Estimated Pressure Errors

Transducer	Pressure Range mm Hg	Estimated Pressure Error mm Hg
0 - 15B	740 - 300	± 7
0 - 15A	360 - 170	± 7
0 - 10	230 - 90	± 5
0 - 5B	100 - 30	± 2.5
0 - 5A	40 - 10	± 2.5
0 - 2	15 - 0	± 1
Differential	± 25	± 0.2

of alcohol. During the initial calibrations of the differential transducer, it was determined that the calibration was essentially invariant with absolute pressure level. Thus, the later calibrations were made using approximately room pressure as the reference pressure. The pressure range covered by the differential transducer and its estimated error are shown in Table 1.

Ascent Run.--For an ascent run the test section, comprised of the test tube and sensing volume, was separated from the tank section by extending the piston, shown in Figure 2, until the piston orifice was to the left of the O-ring, located on the right side of the cylinder. The test section remained at atmospheric pressure while the tank section was pumped down to approximately 1 mm Hg absolute. The actual run was begun by starting the synchronous motor and thus setting the cam in motion. When the pressure in the test section and tank section had equalized, the run was terminated. Three different arrangements of the gear train were used to simulate the three ascent trajectories used in this experiment. These trajectories are shown in Figure 3.

Descent Run.--The preparation for a descent run was similar to that for an ascent run, except that the tank section was pressurized to 500 mm Hg gauge pressure and the test section was pumped down to about 0.1 mm Hg absolute. The descent run was initiated in the same way as the ascent run. When the input pressure reached atmospheric, the tank section was clamped off to prevent damage to the absolute transducers. Five descent trajectories were simulated by experimentally adjusting the gear train. These trajectories are shown in Figure 4.

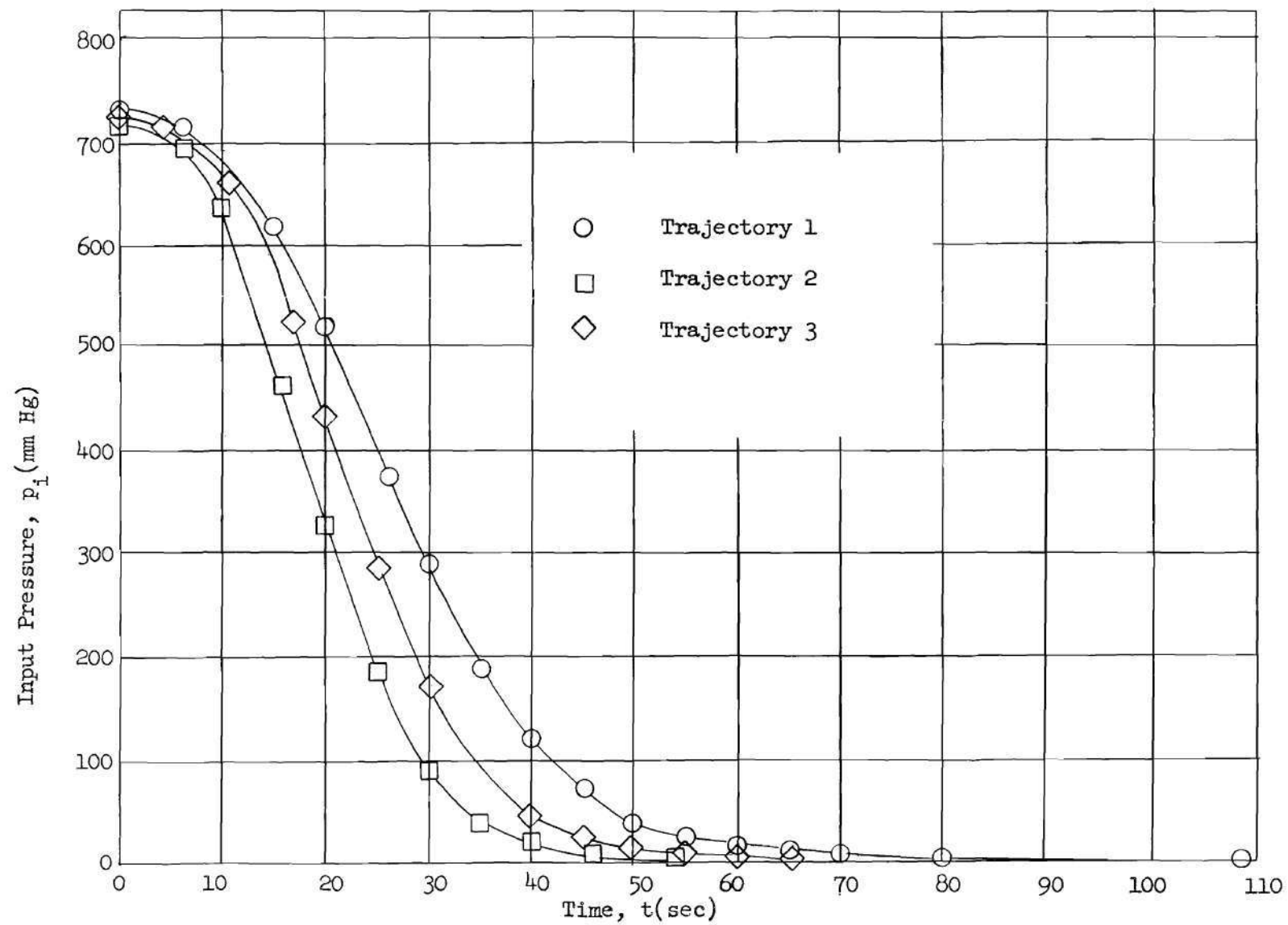


Fig. 3. Typical Continuous Ascent Trajectories.

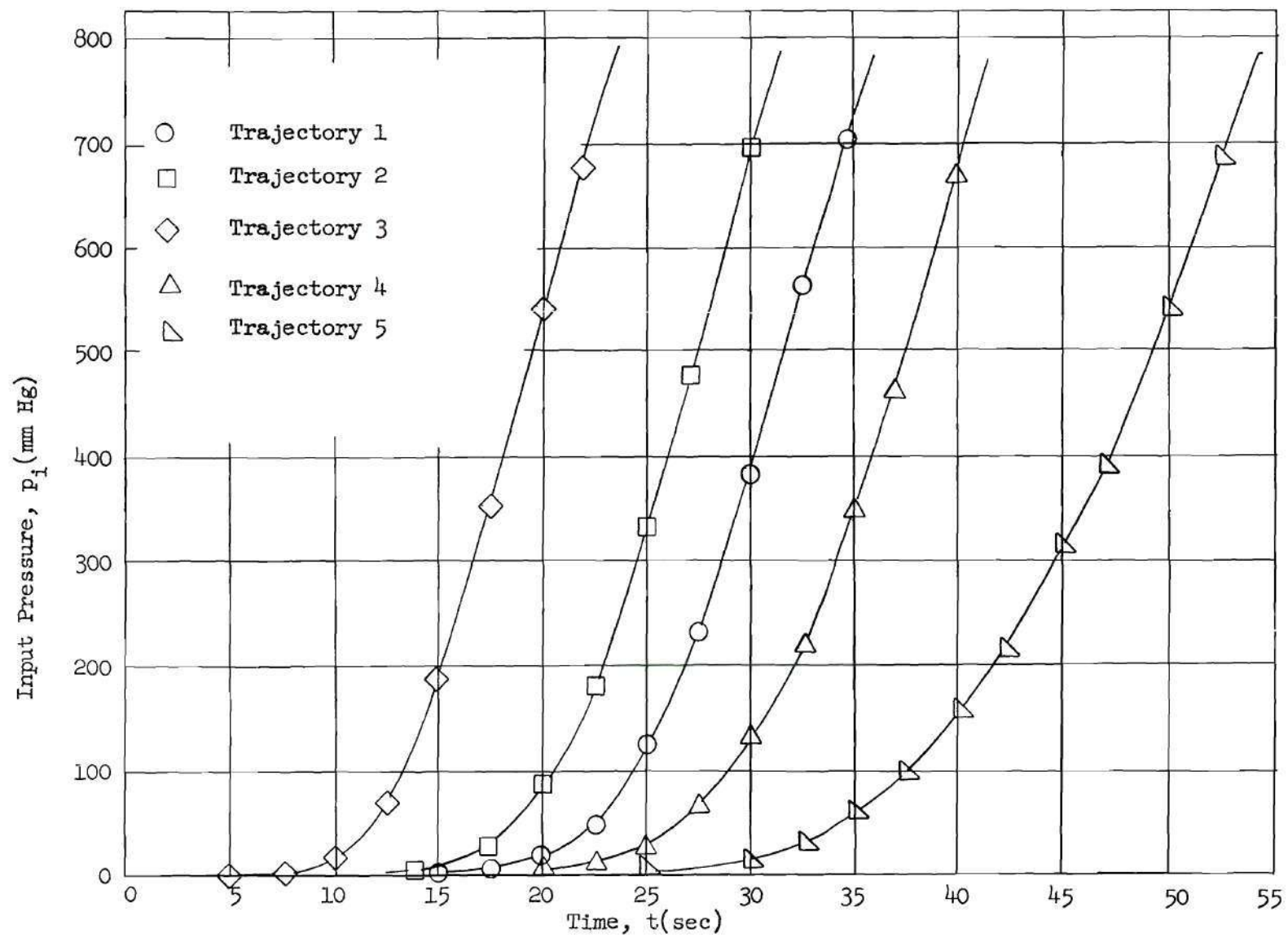


Fig. 4. Typical Continuous Descent Trajectories.

Data Reduction.--Figure 5 represents a typical oscillograph descent record, showing the overlap of the transducer traces and the useful range for each individual trace. The timing lines have been omitted in Figure 5 for reasons of clarity. The reduction of the data starts at Point I in Figure 5. This point represents the equilibrium vacuum pressure in the test system before the run commences. The equilibrium pressures between 0.25 mm Hg absolute and 1.0 mm Hg absolute were monitored by means of an electronic vacuum gauge, which was calibrated against a McLeod gauge. The accuracy of this measurement is within 30 microns. Beginning with Point I, which is known, the value of the pressure in counts is measured along the 0-2 transducer trace until Point II now becomes the starting point, Point III, for the measurement of pressure along the 0 - 5A transducer trace. The 0 - 5A trace is then followed to Point IV, which, as before, becomes the value of the starting point, Point V, for the 0 - 5B trace and so on for the remaining traces. The values of pressure in counts were converted to pressure in mm Hg using the appropriate calibration curves. This method of data production and reduction resulted in errors estimated to be less than one per cent of the absolute pressure at any level of absolute pressure. However, the gain in overall sensitivity and accuracy more than compensated for this one per cent error. Ascent data were reduced in an identical manner in that the data were reduced starting at the lowest equilibrium vacuum pressure and working backward on the oscillograph charts.

The differential pressure between the input end of the line and sensing volume was measured by means of a ± 0.5 psi differential transducer. A typical differential trace is also shown plotted in Figure 5.

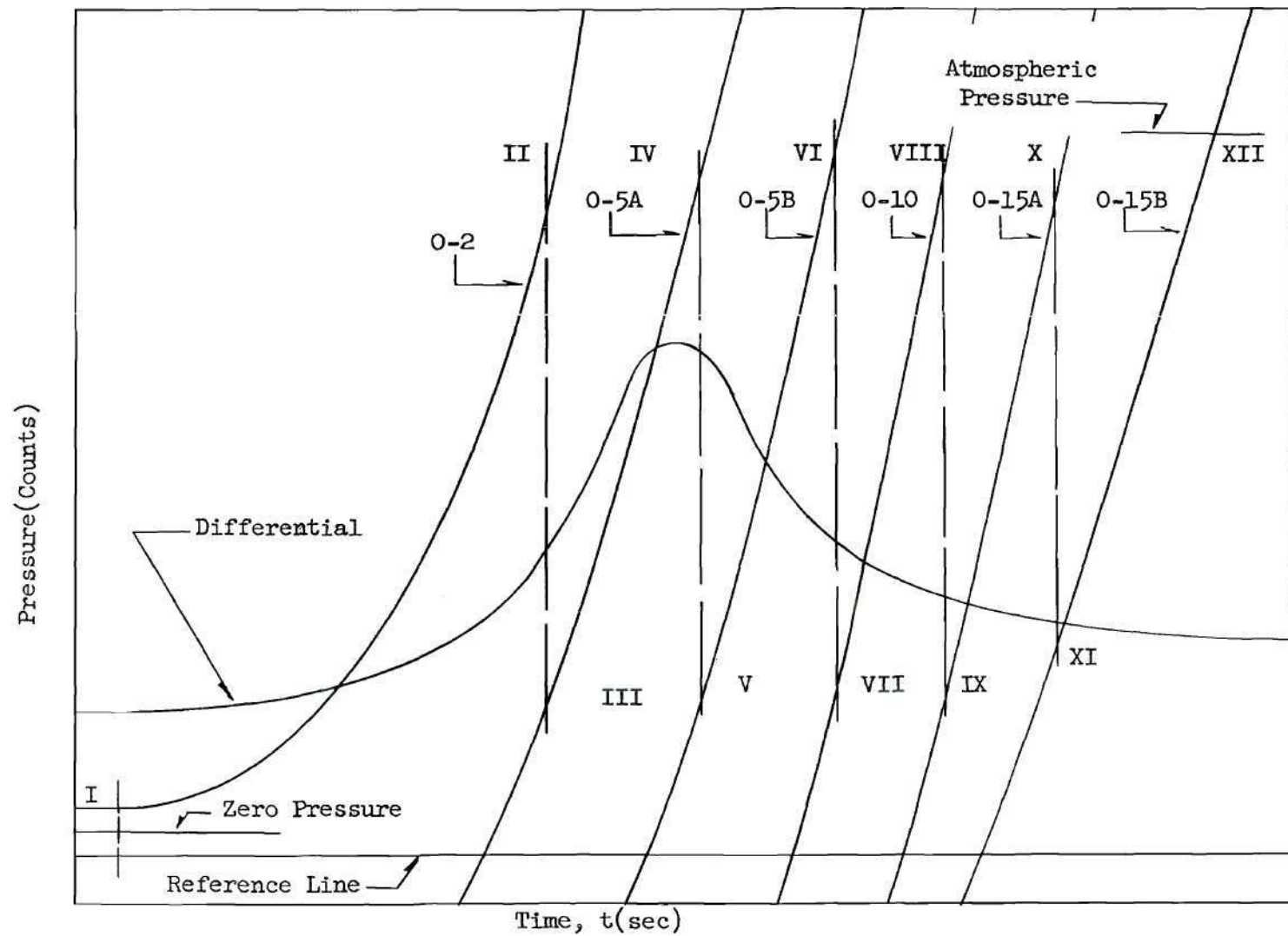


Fig. 5. Typical Descent Oscillograph Record.

Accuracy.--The error in the experimental data is essentially that of accuracy and repeatability of calibrations from day to day, plus the human error in reading the oscillograph records. The maximum errors in the absolute pressure gauges are estimated to be of the order of $\pm 1/2$ per cent of full scale. The calibrations of the absolute pressure transducers indicate that the maximum deviations from the mean are also of the order of $\pm 1/2$ per cent of full scale. The readability of the data from the oscillograph records resulted in maximum errors of the order of $\pm 1/4$ per cent of full scale. On the basis of these errors, it is estimated that the maximum error for the absolute transducers was of the order of ± 1 per cent of the range used for each transducer.

The component errors in the differential transducer were estimated as: the differential calibration, $\pm 1/2$ per cent of full scale; the alcohol manometer, ± 0.06 mm Hg; and reading error, $\pm 1/4$ per cent of full scale.

Table 1 is also presented as a summary of the estimated errors in the experimental data.

CHAPTER IV

RESULTS

In order to attempt to correlate the theory developed in Reference 5 with the experimental data gathered in this investigation, the parameter K in the following equation was determined from the experimental data.

$$\frac{dp_r}{dt} = K(p_i^2 - p_r^2) \quad (4)$$

The procedure for determining K consisted of taking the measured data from a given geometric set-up and a given trajectory and computing K from Equation (4) at several different randomly selected time points. For any given run at least five values of K, corresponding to five different time points, were computed. An arithmetic average of the factor K was then computed for each run. This procedure for determining K was necessary because the values of K varied slightly at different time points on a particular run. This variation is due to scatter in the experimental data and possibly to a variation of K with input to response pressure ratio, $\frac{p_i}{p_r}$. An attempt was made to investigate the effect of pressure ratio on the value of K, but the inherent scatter in the experimental data made it impossible to detect any definite trend.

Equation (3) suggests that the experimentally determined values of K can be correlated with the geometric parameter LV/d^4 , independent of the particular trajectory used to determine K. Thus, all the values

of K were plotted versus the geometric parameter, $\emptyset = \frac{LV}{10^4 d^4}$, in Figure 6. The factor 10^{-4} appearing in the geometric parameter, \emptyset , is merely a convenience. It is again noted that each circled point in Figure 6 represents the arithmetic mean of at least five empirically determined values of K . Also shown on Figure 6, as a broken line, is a plot of the theoretical value of K versus the geometric parameter, \emptyset . The theoretical equation for K from Equation (3) is

$$K = \frac{\pi d^4}{256 \mu VL} \quad (5a)$$

or

$$K = \frac{9.4}{\emptyset} \left(\frac{1}{\text{mm sec}} \right) \quad (5b)$$

using standard values for the constants in Equation (5a).

The solid line in Figure 6 represents a curve faired through the experimental points. The equation of this curve was determined to be

$$K = 9.4 \emptyset^{-\left(1 + \frac{3.25}{\emptyset}\right)} \quad (6)$$

where again K has the units $\left(\frac{1}{\text{mm sec}}\right)$.

Kowalsky (Reference 6) has experimentally determined the pneumatic pressure lags for geometric systems similar to the ones used in this experiment, that are subjected to impulse-type input pressure functions. Values of K were determined from the data of Reference 6 and it is noted that these values are in excellent agreement with the empirical curve shown in Figure 6.

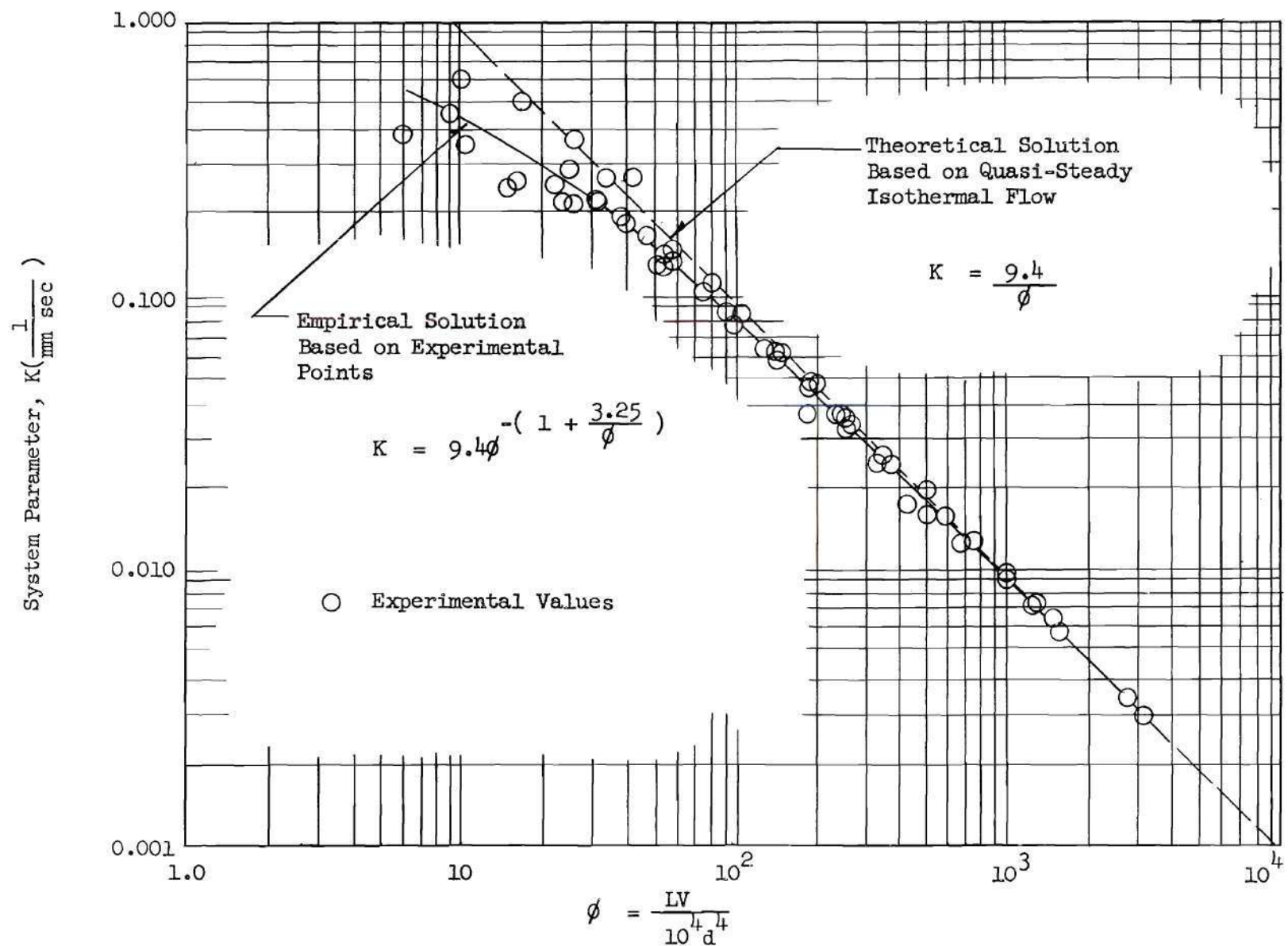


Fig. 6. System Parameter, K , as a Function of Geometric Parameter, ϕ .

From Figure 6 it is noted that the theoretical and empirical values of K agree very closely for values of $\phi > 400$. However, as the value of ϕ decreases below 400, the theoretical and empirical values of K start to deviate. This deviation between the empirical and theoretical values of K as ϕ is reduced is thought to result from the breakdown of the fully-developed flow assumption. Since small values of ϕ can be associated with large line inside diameters, then, for two lines of the same length, the configuration with the smaller L/d would tend to violate the idea of a fully-developed flow over the entire tubing length. The result would be a larger pressure drop, which is indicated by the empirical value of K being lower than its theoretical counterpart.

Figures 7 through 11 represent the correlation of experiment with theory for a representative cross section of system geometries and input pressure functions used in this experiment. To calculate the theory, represented by the solid line on the figures, first the value of ϕ was determined for the particular geometric arrangement and the value of K was calculated from Equation (6). Using this value for K , Equation (4) was solved for $\Delta p = p_i - p_r$ by the method of step by step integration using the initial conditions that

$$p_i(0) = p_r(0)$$

$$p_r'(0) = 0$$

The agreement between experiment and theory represented on Figures 7 through 11 is definitely acceptable.

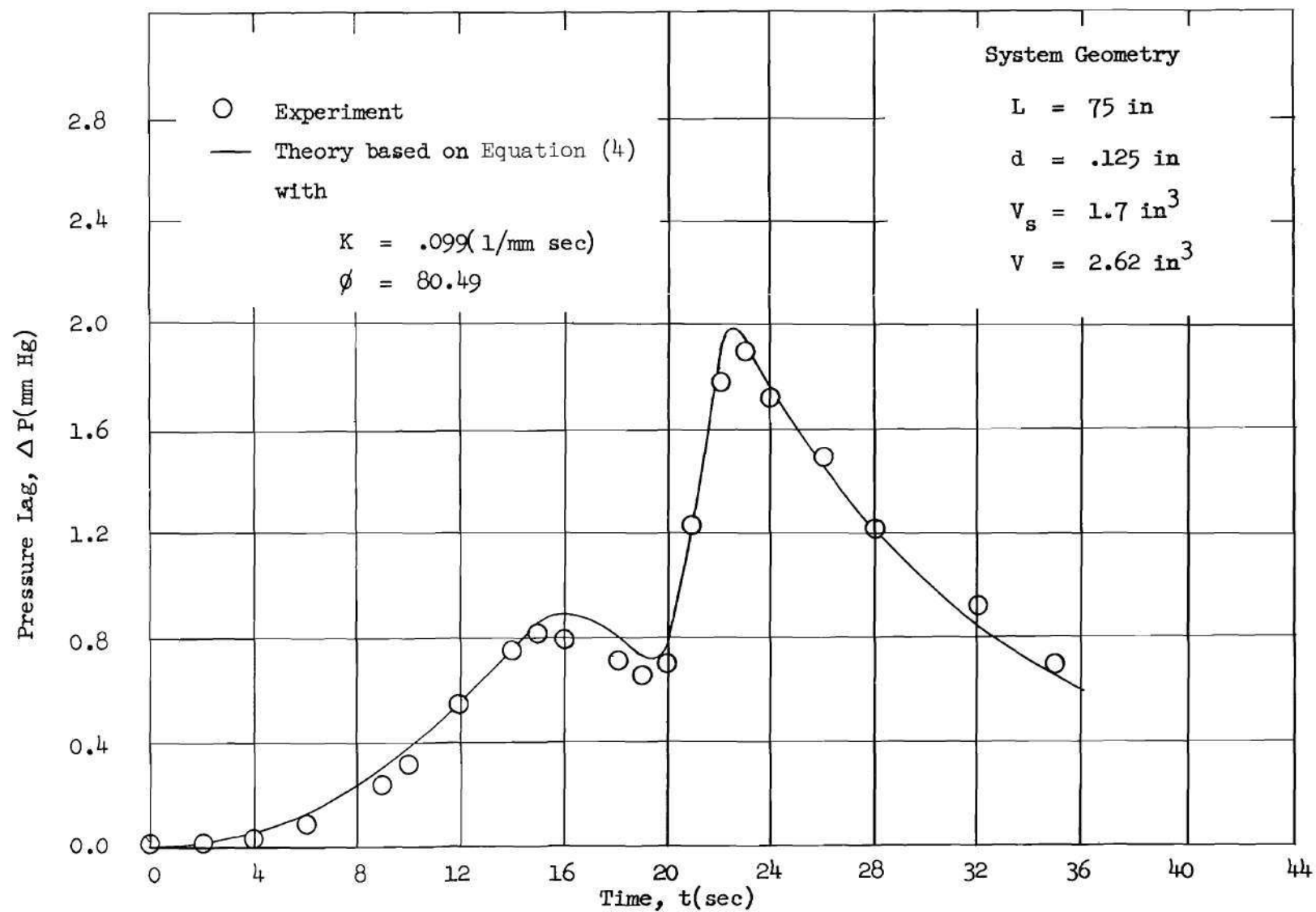


Fig. 7. Correlation of Experiment with Theory for Continuous Descent Trajectory No. 3.

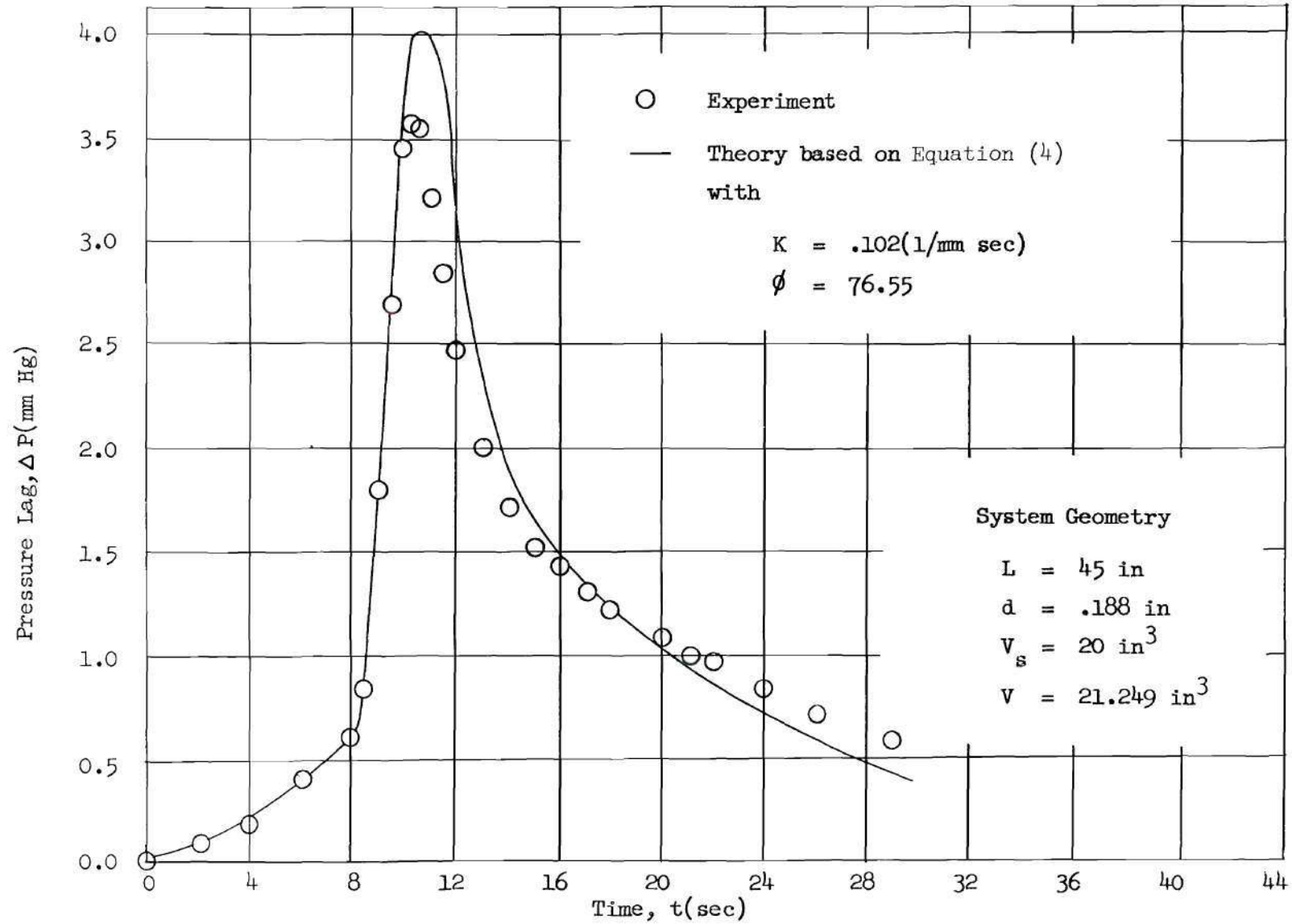


Fig. 8. Correlation of Experiment with Theory for Continuous Descent Trajectory No. 3.

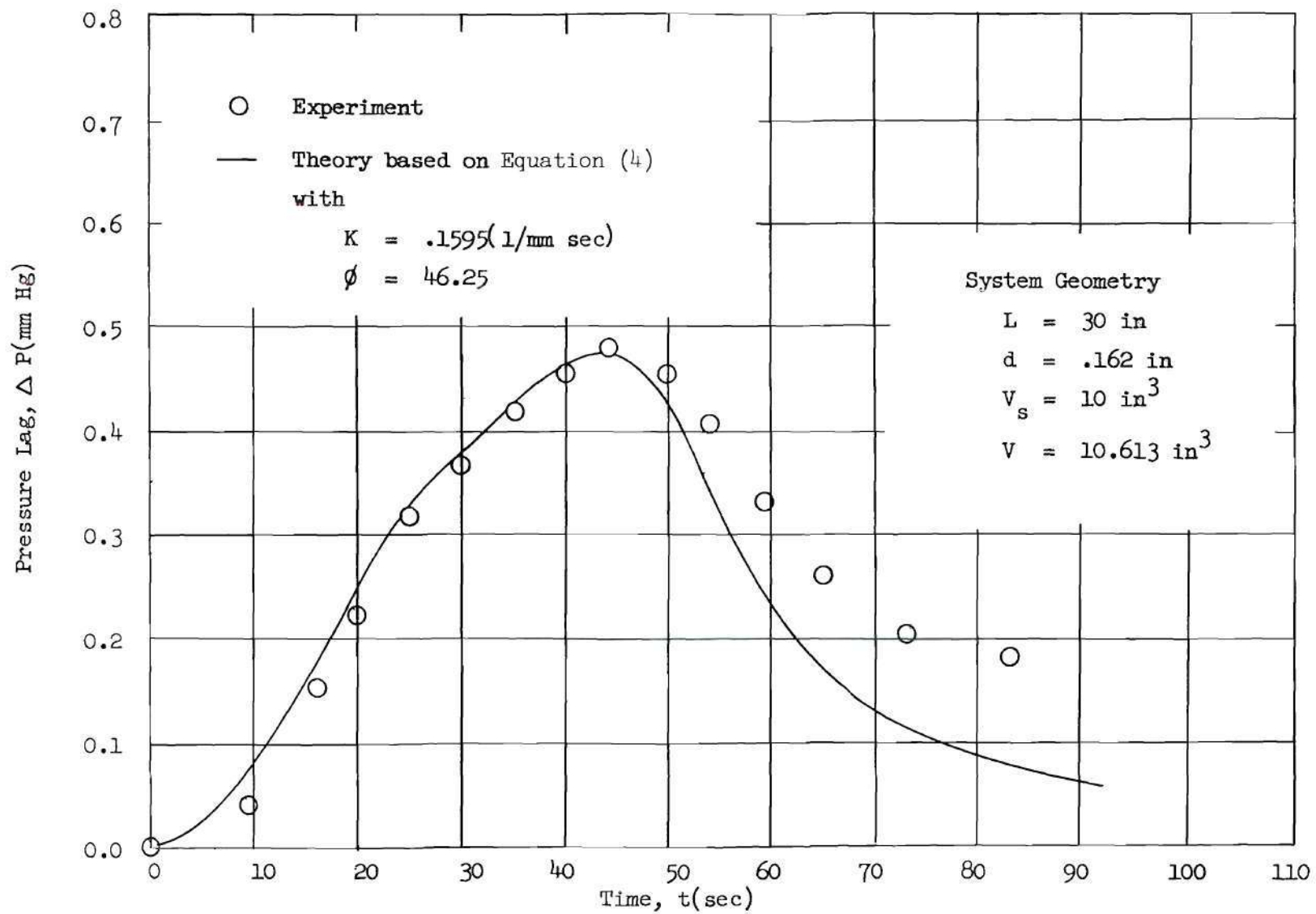


Fig. 9. Correlation of Experiment with Theory for Continuous Ascent Trajectory No. 2.

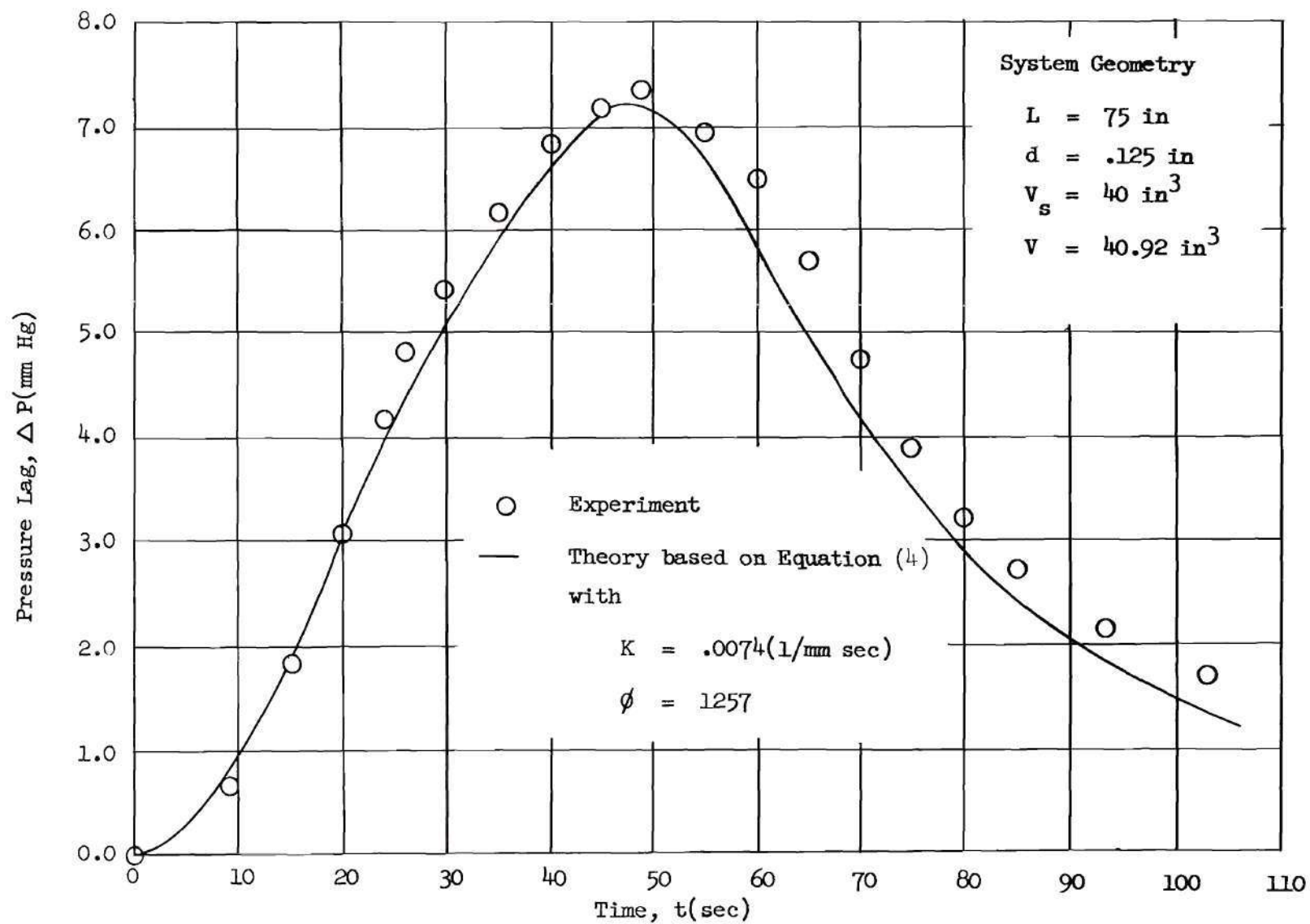


Fig. 10. Correlation of Experiment with Theory for Continuous Ascent Trajectory No. 3.

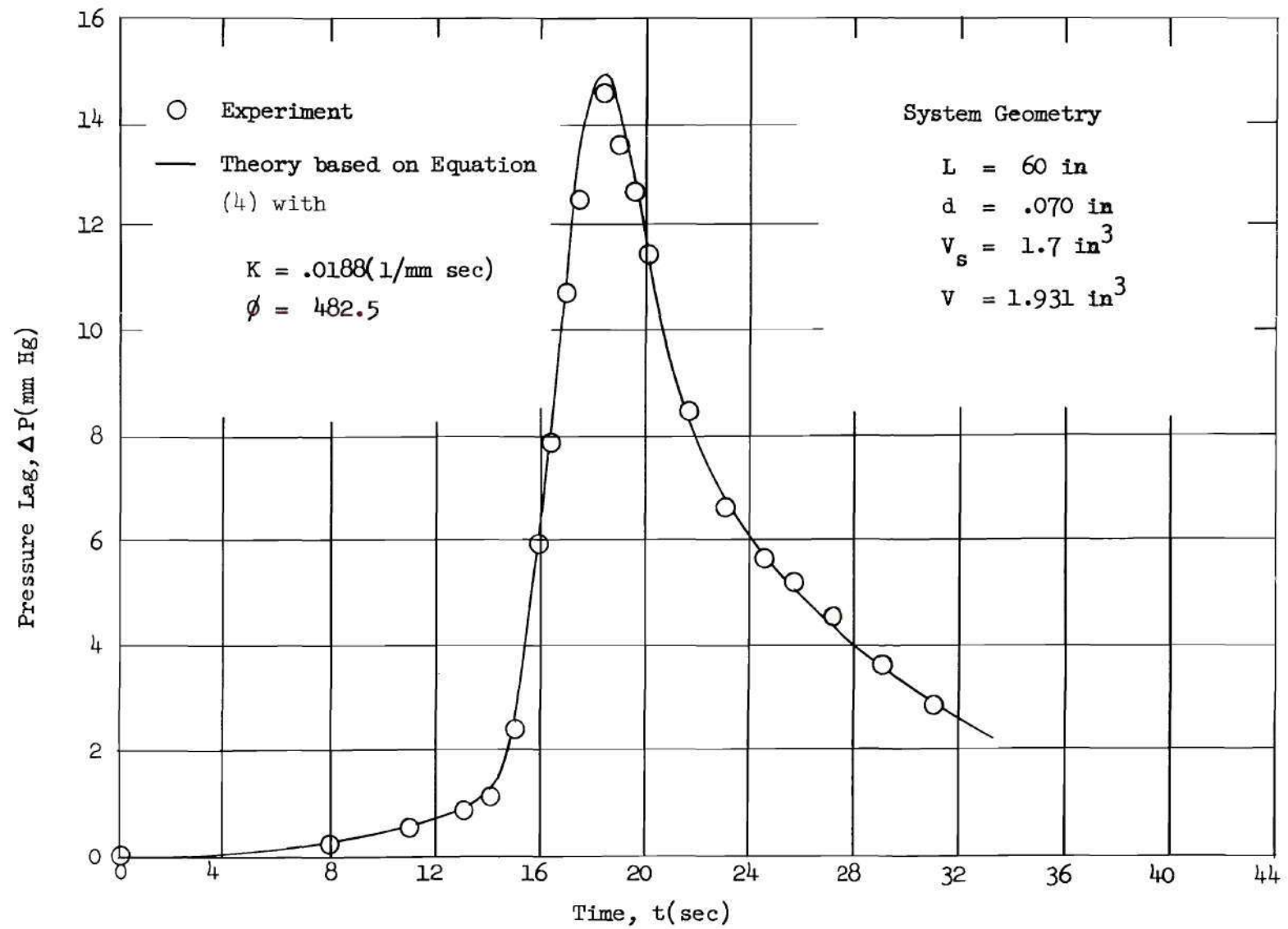


Fig. 11. Correlation of Experiment with Theory for Continuous Descent Trajectory No. 3.

CHAPTER V

CONCLUSIONS

The results of this analysis, under the restriction of the range of parameters tested, are considered applicable for the prediction of pneumatic pressure lag in missile plumbing systems. The necessity of the empirical determination of the parameter, K , probably results from the failure of the fully-developed flow assumption being available over the entire tube length for those configurations where L/d is small. The analysis shows that the parameter K is independent of trajectory and depends only on the system geometry. The experimental data show that, for the small pressure lags encountered in this experimentation, the value of K is essentially independent of pressure ratio, $\frac{p_i}{p_r}$. The definition of K indicates that the pneumatic lag for a given trajectory can be minimized if the geometric ratio, $\frac{LV}{d^4}$, is minimized.

CHAPTER VI

RECOMMENDATIONS

In order to complete the study of pressure lags inherent in ballistic missile plumbing systems, the following recommendations are made:

1. Additional experimental data should be obtained for a greater range of system variables (i.e., line length, line diameter, and sensing volume.)
2. The effect of high inlet temperatures should be determined.
3. The effect of connector fittings, with inside diameters smaller than the line diameter, should be investigated.
4. The effect, if any, of pressure ratio, $\frac{p_i}{p_r}$, on K should be determined.

REFERENCES

1. Huston, W. B., Accuracy of Airspeed Measurements and Flight Calibration Procedures, National Advisory Committee for Aeronautics, N A C A TN 1605, June, 1948.
2. Wildback, W. A., Pressure Drop in Aircraft Installations, National Advisory Committee for Aeronautics, N A C A TN 593, February, 1937.
3. Delio, G. L., Schwent, G. V., and Cesaro, R. S., Transient Behavior of Lumped-Constant Systems for Sensing Gas Pressures, National Advisory Committee for Aeronautics, N A C A TN 1988, December, 1949.
4. Vaughn, H., Experimental and Analytical Methods for Determining the Pressure and Time Lag in Pressure-Measuring Systems, Sandia Corporation, SC - 3244 (TR), Albuquerque, New Mexico, May, 1954.
5. Ducoffe, A. L., A Theoretical and Experimental Study for the Prediction of Pneumatic Pressure Lag Inherent in Typical Ballistic Missile Plumbing Systems, Georgia Institute of Technology Research Station, Final Report, Project A - 369, Atlanta, Georgia, August, 1959.
6. Kowalsky, B. D., An Experimental Study for the Prediction of Pressure Lag Inherent in Ballistic Missile Plumbing Systems When Subjected to Impulse-Type Pressure Functions, Unpublished Master's Thesis, Georgia Institute of Technology, Atlanta, Georgia, April, 1959.